Journal of Medicinal Chemistry

pubs.acs.org/jmc

Article

GMP Compliant Synthesis of [^{18}F]Canagliflozin, a Novel PET Tracer for the Sodium−Glucose Cotransporter 2

Sjoukje van der Hoek, Inês F. Antunes, Khaled A. Attia, Olivier Jacquet, Andre Heeres, Marian Bulthuis, Rolf Zijlma, Hendrikus H. Boersma, Harry van Goor, Ton J. Visser, Hiddo J. L. Heerspink, Philip H. Elsinga, and Jasper Stevens*

Cite This: *J. Med. Chem.* 2021, 64, 16641−16649

Read Online

ACCESS | Metrics & More | Article Recommendations | Supporting Information

ABSTRACT: Inhibition of the sodium−glucose cotransporter 2 (SGLT2) by canagliflozin in type 2 diabetes mellitus results in large between-patient variability in clinical response. To better understand this variability, the positron emission tomography (PET) tracer [^{18}F]canagliflozin was developed via a Cu-mediated ^{18}F-fluorination of its boronic ester precursor with a radiochemical yield of 2.0 ± 1.9% and a purity of >95%. The GMP automated synthesis originated [^{18}F]canagliflozin with a yield of 0.5−3% (n = 4) and a purity of >95%. Autoradiography showed [^{18}F]canagliflozin binding in human kidney sections containing SGLT2. Since [^{18}F]canagliflozin is the isotopologue of the extensively characterized drug canagliflozin and thus shares its toxicological and pharmacological characteristics, it enables its immediate use in patients.

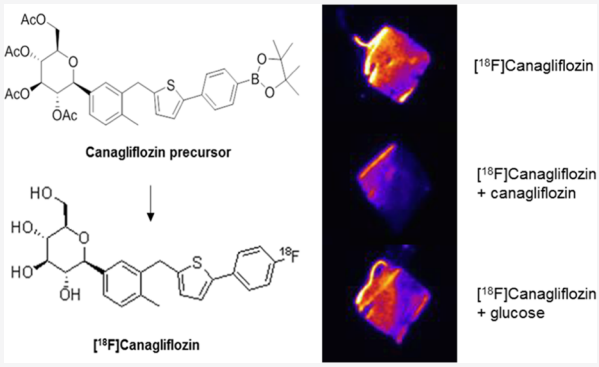

INTRODUCTION

Patients with type 2 diabetes mellitus (T2DM) remain at an increased risk of cardiovascular diseases and chronic kidney diseases[1] despite currently available treatment options. Sodium−glucose cotransporter 2 (SGLT2) inhibitors are clinically available to optimize glycemic control. The SGLT2 is located in the proximal tubules of the kidneys where it reabsorbs filtered glucose. Through inhibition of this transporter, glucose reabsorption is diminished, urinary glucose excretion increases, and consequently plasma glucose levels will decrease.[2] In addition, SGLT2 inhibitors decrease the body weight, blood pressure, and urinary excretion of albumin, a surrogate marker for the progression of kidney disease. Large clinical trials have shown that SGLT2 inhibitors reduce the risks of heart failure and end-stage kidney disease.[3−6]

Despite these clinical benefits at a population level, there is a large variation in drug response. Clinical studies showed that in 20% of patients albuminuria does not improve in response to SGLT2 inhibition.[7] The underlying mechanisms of this individual variation in response to SGLT2 inhibition are unknown.

We hypothesize that differences in drug response can, among others, be explained by variations in the SGLT2 inhibitor tissue distribution and/or changes in the SGLT2 density due to the pathology of the disease. To quantitatively, and preferably noninvasively, investigate the tissue distribution of SGLT2 inhibitors and SGLT2 density in patients, there is a need for a radiolabeled SGLT2 positron emission tomography (PET) tracer. α-Methyl-4-[^{18}F]fluoro-4-deoxy-D-glucopyranoside (Me-4FDG) and [^{11}C]methyl-D-glucoside have been suggested as PET tracers for imaging SGLT.[8,9] However, these tracers are not SGLT2-specific; both are also substrates for SGLT1, and Me-4FDG additionally possesses affinity toward GLUT2.[9,10] The marketed drugs from the SGLT2 inhibitor class, gliflozins, have been proven to be more selective toward SGLT2.[11,12] Recently, 4-[^{18}F]fluoro-dapagliflozin (F-Dapa) was synthesized and subsequently shown to exhibit subtype selectivity toward SGLT2.[13] However, due to the addition of an ^{18}F-fluoro group to dapagliflozin, F-dapa does not retain the original molecular structure of the marketed drug dapagliflozin. It may, as a result, exhibit different pharmacokinetic and pharmacodynamic properties.

Therefore, our aim was to synthesize a PET tracer with a molecular structure identical to one of the currently marketed SGLT2 inhibitors, as this would also retain the biochemical properties of the drug. An additional benefit is that the PET tracer can be used immediately in human studies without extensive toxicity testing. We preferred an ^{18}F-labeled tracer because of its favorable physical and nuclear characteristics for

Received: July 16, 2021
Published: November 8, 2021

https://doi.org/10.1021/acs.jmedchem.1c01269
J. Med. Chem. 2021, 64, 16641−16649

Scheme 1. Synthetic Strategy toward Canagliflozin Precursor

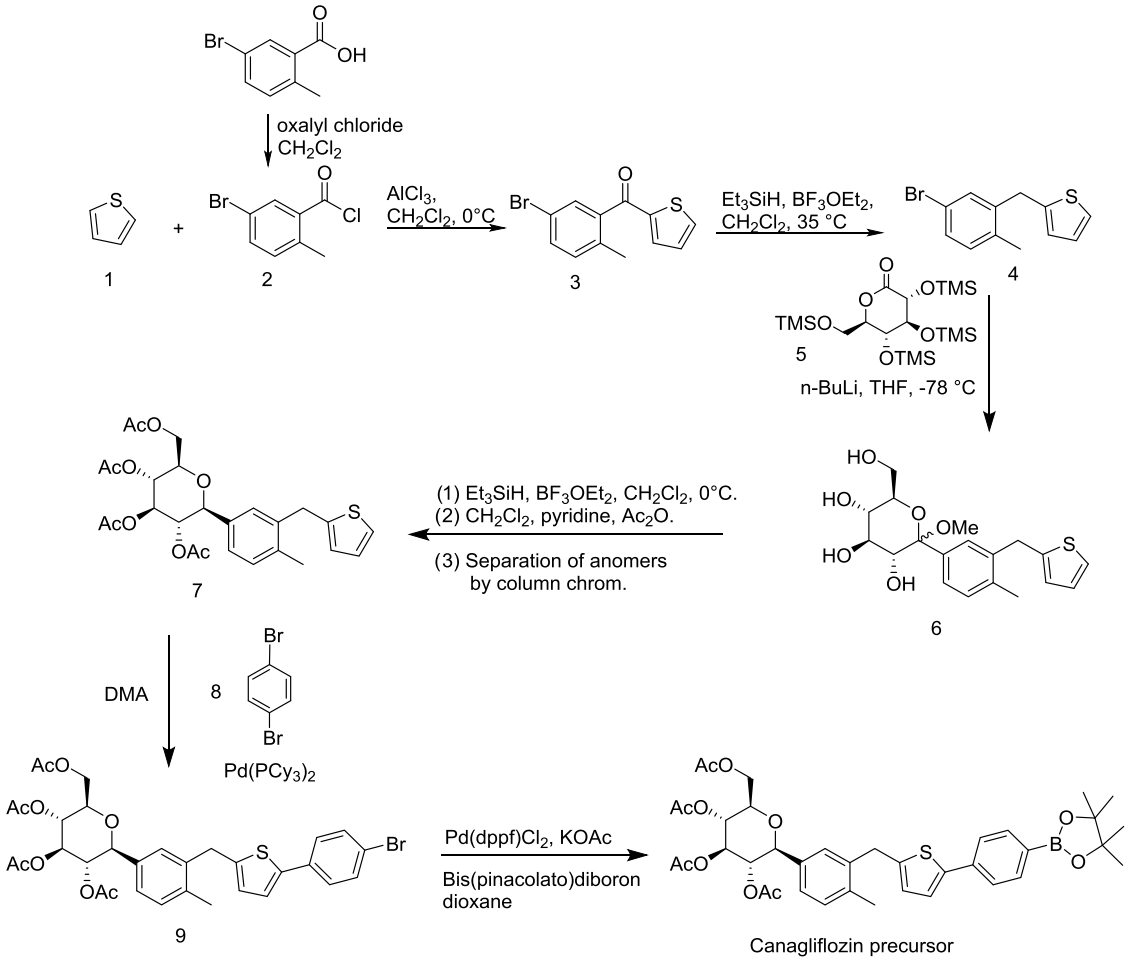

PET imaging. Within the drug class of (marketed) SGLT2 inhibitors, only canagliflozin contains a fluorine atom that can be replaced by an ^{18}F-radionuclide. In this study, we describe the synthesis of [^{18}F]canagliflozin and its precursor, as well as its in vitro affinity toward SGLT2.

RESULTS AND DISCUSSION

Chemistry. Canagliflozin precursor equipped with a pinacol aryl boronic ester moiety has been successfully prepared and its synthesis is depicted in Scheme 1. The route is inspired by the work of Meng et al.[14] and Nomura et al.[11] Whereas Nomura used 2-substituted thiophenes in the "Friedel−Crafts" acylation reaction, we started from the unsubstituted thiophene. In the final steps, canagliflozin precursor was prepared by a Pd-catalyzed thiophene−aryl coupling reaction via the C−H bond activation followed by a Miyaura borylation reaction by cross-coupling of bis(pinacolato)diboron (B_2pin_2) with the aryl halide.[15]

Briefly, the synthesis started with the coupling of thiophene **1** with acid chloride **2** (prepared by the reaction of 5-bromo-2-methylbenzoic acid with oxalyl chloride) through a Friedel−Crafts reaction in an 86% yield. Initial attempts to reduce the ketone functionality in compound **3** with triethylsilane and BF_3.OEt_2 at 0 °C gave **4** albeit in a low yield (25%, data not shown). At this temperature, a dimeric byproduct was formed. This was circumvented by warming the reaction mixture at 35 °C after addition of the reducing agents (triethylsilane/BF_3·Et_2O), forming intermediate **4** with an improved yield of 77%. Delta-gluconolactone was protected with trimethylsilyl chloride to yield **5** in 92%. To prevent the organolithium intermediate to be quenched by the moisture present in compound **5**, it is of utmost importance that compound **5** is dry. This was achieved by stripping the product a few times with toluene. Silylated gluconolactone **5** was then reacted with **4** to afford **6** as a mixture of α- and β-anomers in a 49% yield. The anomers were not separated at this stage.

When the hydrosilylation on **6** was performed on a small scale (200 mg) at 0 °C, a selectivity α/β of 1:5 was obtained. However, when the reaction was scaled up to 18 g, the selectivity dropped to 1:2. This drop in selectivity is most likely due to the much larger exothermic effect observed on this scale during the addition of boron trifluoride to the reaction mixture. Nevertheless, after acetylation of the crude product and purification by column chromatography, pure β-**7** anomer was isolated in a 39% yield.

Pure β-**7** anomer was then reacted with an excess of dibromobenzene (**8**) via a Pd-catalyzed thiophene−aryl coupling reaction via the C−H bond activation using $(Cy_3P)_2Pd(0)$ as catalyst (20%) to afford intermediate **9** in a 31% yield. Finally, the canagliflozin precursor was synthesized by borylation of **9** using bispinacolatodiboron and Pd(dppf)Cl_2 (5%) as catalysts in an 86% yield after purification. Thus, this multistep procedure proved to be successful and gave the desired borylated-canagliflozin precursor in multigram amounts.

https://doi.org/10.1021/acs.jmedchem.1c01269
J. Med. Chem. 2021, 64, 16641−16649

Scheme 2. Radiosynthesis of [^{18}F]Canagliflozin

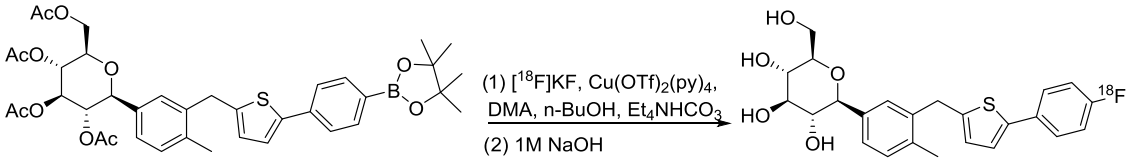

Canagliflozin precursor [^{18}F]Canagliflozin

Table 1. Results of Production Process and Quality Control

[^{18}F]canagliflozin	specification	validation 1	validation 2	validation 3
appearance	clear, colorless	yes	yes	yes
pH	5−8	6.5	7.0	6.5
filter integrity: pressure hold test	>1.8 bar	>1.8	>1.8	>1.8
bubble point test[a]	<10% reduction of pressure	<10	<10	<10
	>2.8 bar	N/A	N/A	N/A
identity	retention time ≤ 0.4 min compared to standard	yes	yes	yes
radiochemical purity	≥95%	100	100	100
unknown impurities	<1 mg/L	<1.0	<1.0	<1.0
-canagliflozin LOQ[b] = 0.4 mg/L	<1 mg/L	<0.4	<0.4	<0.4
-canagliflozin precursor	<1 mg/L	<0.1	<0.1	0.6
molar activity EOS: [^{18}F]canagliflozin	≥10 000 GBq/mmol	>23 000	>47 000	>52 000
activity yield	>200 MBq (standard dose)	232	466	524
sterility	sterile	sterile	sterile	sterile
osmomolarity	<2250 mosmol/kg	1690	1820	1760
acetonitrile	<410 mg/L	17.7	14.8	10.1
DMA	<1090 mg/L	<50	<50	<50
ethanol	<100 g/L	62.8	68.7	65.8
propanol	<5000 mg/L	<100	<100	<100
copper	<50 mg/L	<1	<1	<1
TEAHC[c]	<260 mg/L	<260	<260	<260
endotoxins	<2.5 EU/mL	<0.05	<0.05	<0.05

[a]With a failing pressure hold test, the bubble point test needs to be done after radioactive decay. [b]Limit of quantification. [c]Tetraethylammonium hydrogen carbonate.

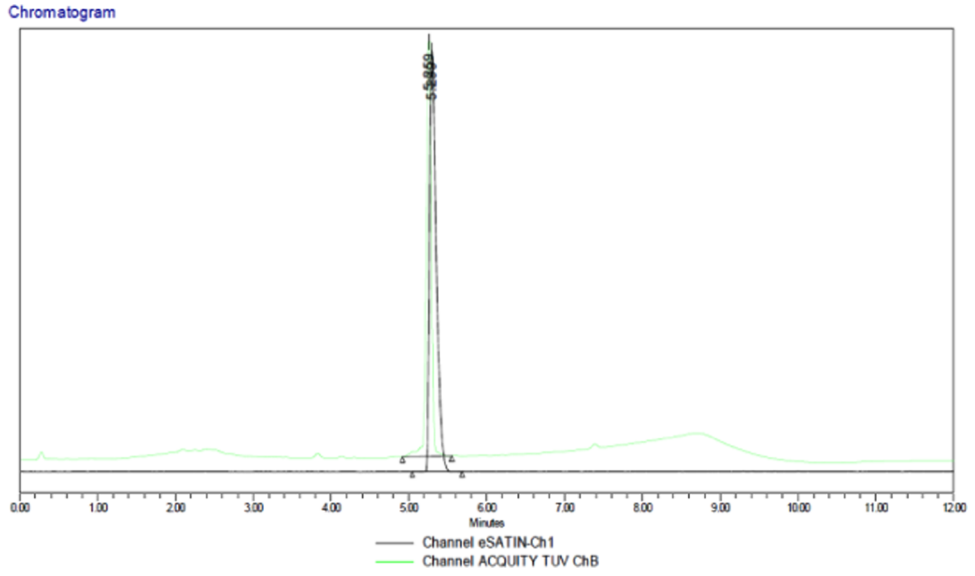

Figure 1. UPLC chromatogram from the final product [^{18}F]canagliflozin (black: γ detector, green: UV detector). The final product had the same retention time compared to the commercially available nonradioactive-labeled reference standard.

Radiochemistry. The production of ^{18}F-arenes through the copper-mediated oxidative ^{18}F-fluorination from pinacol-derived aryl boronic esters (arylBPin), upon treatment with [^{18}F]KF/K2.2.2 and $Cu(OTf)_2(py)_4$, has shown to be a robust synthesis method.[16,17] This method tolerates electron-poor and electron-rich arenes and various functional groups. Therefore, this strategy would be most suitable for the radiosynthesis of [^{18}F]canagliflozin from the borylated precursor.

https://doi.org/10.1021/acs.jmedchem.1c01269
J. Med. Chem. 2021, 64, 16641−16649

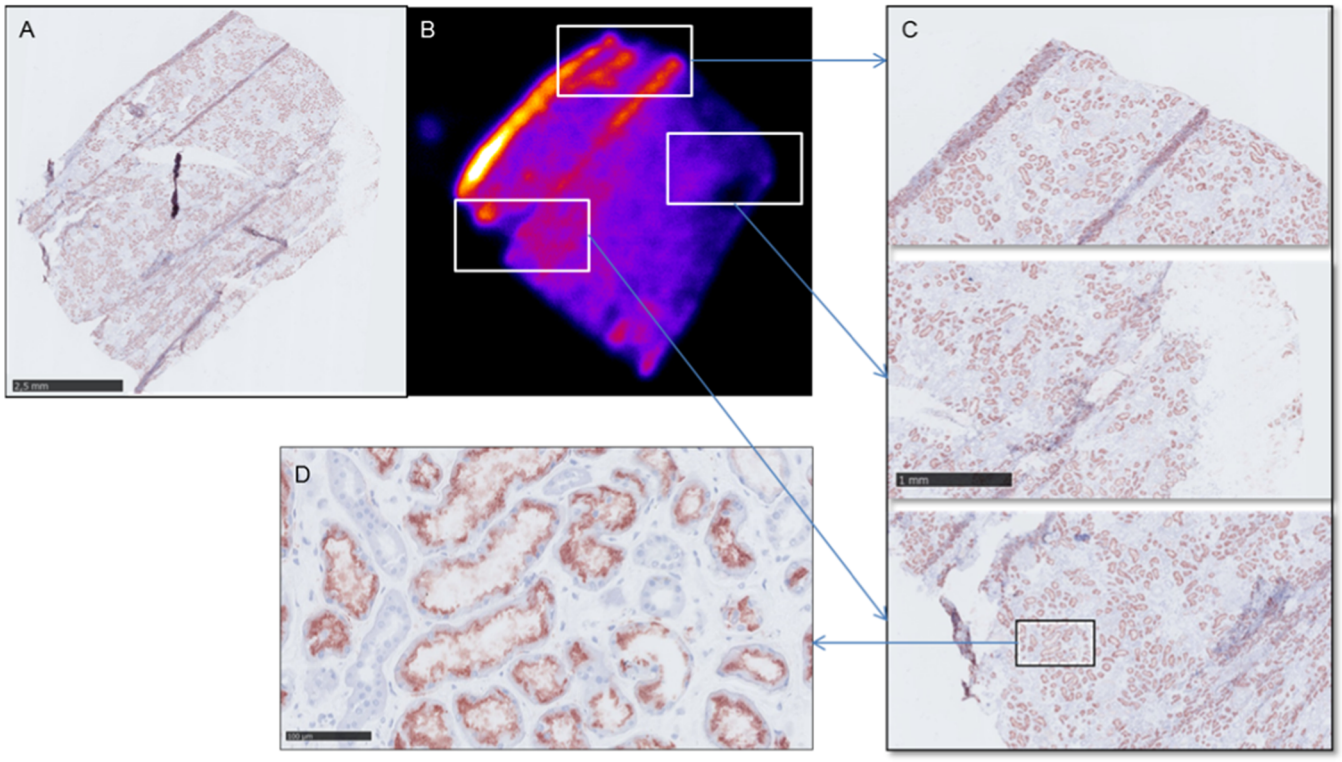

Figure 2. SGLT2 distribution, as shown with immunohistochemistry on the luminal side of proximal tubules in a human kidney slice (A, C, and D: scanning was performed with a 40× magnification lens, and scale bars indicate 2.5 mm, 1 mm, and 100 μm, respectively), compared to [^{18}F]canagliflozin binding on an adjacent kidney slice obtained via autoradiography (B).

Typically, in copper-mediated oxidative ^{18}F-fluorinations of aryl boronic esters, the most common Cu-catalyst used is $Cu(OTf)_2(py)_4$.[18−21] Where most of the reactions were found to be optimal at 120 ± 10 °C, either in dimethylacetamide or in DMF, the former solvent gave a better conversion efficacy after 20−30 min of reaction time.[22] This method was applied in the synthesis of [^{18}F]canagliflozin with a final radiochemical yield of 2.0 ± 1.9% (n = 12) within 90 min, as depicted in Scheme 2.

An automated program was created to synthesize [^{18}F]-canagliflozin in a Modular-Lab PharmTracer Eckert and Ziegler cassette-based synthesis module, which is suitable for the GMP compliant production of PET tracers (Supporting Information Figure S3). For automated synthesis, some small adjustments were made. n-Butanol being highly viscous was mostly lost in the plastic tubes of the automated synthesizer. This led to very low yields to no product. Thus, this was replaced with a less viscous solvent, 2-propanol, and [^{18}F]canagliflozin could be produced with a final yield of 0.5−3.0% (n = 4) and a consistent quality complying with all predefined specifications, as described in Table 1 (see the Supporting Information for optimization of the reaction conditions).

Despite the relatively low yield, the automated synthesis was found to be robust and stable under different conditions (Supporting Information "Pilot experiments"), yielding at least 200 MBq of formulated pure [^{18}F]canagliflozin with a molar activity higher than 10 GBq/μmol and a radiochemical purity of >95%, with a starting activity of 100 GBq (Figure 1), ready for patient injection.

In Vitro Binding Experiments with Autoradiography. The advantage of our labeling strategy is that [^{18}F]canagliflozin retains the chemical structure of canagliflozin and therefore also its high selectivity for the SGLT2 (in vitro IC_{50} for hSGLT1, hSGLT2, and GLUT1, respectively, at 910, 2.2, and >1000 nM[11]). To confirm the binding of [^{18}F]canagliflozin to SGLT2, human kidney samples taken from cortical areas, corresponding with the known anatomical localization of the SGLT2, were used and compared to staining of the SGLT2 with immunohistochemistry (IHC). As depicted in Figure 2, autoradiography showed tracer binding diffusely over the slices corresponding with the pattern of SGLT2 distribution by IHC. By combining autoradiography with IHC, we were also able to demonstrate that the areas with extreme [^{18}F]canagliflozin binding (yellow areas in Figure 2B) were caused by the folded tissue on the slice, whereas areas that completely lack [^{18}F]canagliflozin binding were the result of the missing tissue on the slice.

In addition, in the presence of an excess of canagliflozin, the binding of [^{18}F]canagliflozin was significantly reduced (52.1 ± 8.1%, p < 0.0001, n = 6; Figure 3A) and there was a trend toward reduced binding of [^{18}F]canagliflozin when the nonspecific biological substrate of the SGLT2 glucose (22.6 ± 25.1%) (p = 0.2598, n = 3; Figure 3B) was added (in vitro K0.5 = 4.9 mM[23]).

Together, these experiments confirm that [^{18}F]canagliflozin binds to the SGLT2. Without the requirement for toxicity testing, [^{18}F]canagliflozin is directly suitable for clinical studies. The "Canagliflozin REnal Distribution Intervention Trial" (CREDIT) is planned to assess the feasibility of [^{18}F]-canagliflozin and quantify, noninvasively, individual differences in target-site exposure in patients with T2DM (Netherlands Trial Register; NL7707).

■ CONCLUSIONS

We showed the successful automated synthesis of the SGLT2 inhibitor [^{18}F]canagliflozin. This tracer showed specificity to the SGLT2 in autoradiography experiments with human kidney

https://doi.org/10.1021/acs.jmedchem.1c01269
J. Med. Chem. 2021, 64, 16641−16649

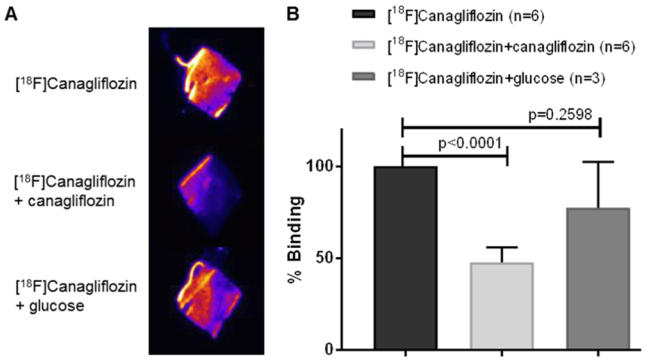

Figure 3. Representative autoradiography images of [^{18}F]canagliflozin binding in human kidney slices incubated with [^{18}F]canagliflozin alone, together with canagliflozin or with glucose (A). Bar graph showing the binding of [^{18}F]canagliflozin in the three different groups presented as a percentage relative to incubation with [^{18}F]canagliflozin alone (B).

slices. Given its unchanged structure compared to the marketed compound, its characteristics and the potential to noninvasively quantify the tissue distribution of canagliflozin and SGLT2 density in humans as determinants of between-patient variability in canagliflozin response can now be studied.

EXPERIMENTAL SECTION

General Procedures: Chemistry and Radiochemistry. All reagents and solvents were obtained from commercial sources (Sigma-Aldrich, Acros, Biosolve, Merck, and Cambridge Isotope Laboratories for deuterated solvents) and used without further purification unless stated otherwise. All reactions were performed in dried glassware under a nitrogen atmosphere. Nuclear magnetic resonance (NMR) spectra were recorded on a Bruker DPX300. The precursor, as well as canagliflozin, possesses a purity of >95% determined by UPLC using an ACQUITY UPLC BEH C18 1.7 μm (2.1 mm × 50 mm) column eluted with a 35:65 aqueous ACN (0.1% TFA)/water (0.1% TFA) as mobile phase at a flow of 0.6 mL/min (λ = 217 nm).

Chemistry. *(5-Bromo-2-methylphenyl)(thiophen-2-yl)-methanone (**3**).* *N*,*N*-Dimethylformamide (2 g, 2 mL, 0.09 equiv, 30 mmol) was added to a suspension of 5-bromo-2-methylbenzoic acid (62.67 g, 1 equiv, 291.4 mmol) in dichloromethane (DCM) (500 mL), and the reaction mixture was stirred for 2.5 h at room temperature until gas evolution ceased. After concentration under reduced pressure, the residue was dissolved in DCM (100 mL) and added, via a dropping funnel at 0 °C over the course of 20 min, to a suspension of aluminum trichloride (42.74 g, 1.1 equiv, 320.6 mmol) in DCM (300 mL), resulting in a dark red coloration. Thiophene (24.52 g, 1 equiv, 291.4 mmol) was slowly added (over 5−10 min), and the reaction mixture was stirred overnight at room temperature. High-performance liquid chromatography (HPLC) confirmed the almost full conversion of thiophene to the desired product. The reaction mixture was quenched slowly at 0 °C with aqueous saturated sodium bicarbonate and then extracted with DCM (3×). The organic layers were washed successively with 1 M hydrochloride (1×) and brine (2×), dried over sodium sulfate, filtered, and concentrated. The heterogeneous mixture was taken up in MTBE (~0.5 L) and filtered through a pad of Celite to remove salts. The cake was washed with MTBE until colorless, and the filtrate was concentrated to dryness to afford **3** (70.3 g, 85.8%) as a brown oil that slowly crystallized upon standing.

^{1}H NMR (300 MHz, chloroform-*d*) δ 7.76 (dd, *J* = 4.9, 1.2 Hz, 1H), 7.56 (d, *J* = 2.2 Hz, 1H), 7.51 (dd, *J* = 8.1, 2.2 Hz, 1H), 7.43 (dd, *J* = 3.8, 1.2 Hz, 1H), 7.22−7.07 (m, 2H), 2.32 (s, 3H).

^{13}C NMR (75 MHz, chloroform-*d*) δ 188.67, 144.20, 140.25, 135.76, 135.53, 135.36, 133.17, 132.72, 130.51, 128.31, 118.78, 19.19.

Mass (HPLC-MS): 282.9 (M + 1).

*2-(5-Bromo-2-methylbenzyl)thiophene (**4**).* Triethylsilane (115.80 g, 0.16 L, 4 equiv, 995.84 mmol) was added at 0 °C to a solution of **3** (70.00 g, 1 equiv, 248.96 mmol) in a 1/1 mixture of DCM/acetonitrile (ACN) (700 mL). Boron trifluoride diethyl etherate (BF_3.OEt_2, 106.00 g, 94.6 mL, 3 equiv, 746.88 mmol) was added over 10−15 min, and the reaction mixture was stirred at 35 °C. At this temperature, the reaction was quite fast and turned from dark to clear orange (heterogeneous). After 45 min, the starting material was fully converted (according to HPLC analysis) and the reaction mixture was cooled down to 0 °C. The reaction was carefully quenched with 2 M potassium hydroxide solution (gas evolution and exothermic). The aqueous layer was extracted with MTBE (3×), the organic layers were washed successively with potassium hydroxide (1×) and brine (2×), dried with sodium sulfate, filtered, and concentrated to afford a crude orange oil. The latter was diluted in a minimum of heptane and purified by automated silica gel chromatography eluted with heptane. The first fractions (bottles 1−10) were concentrated to dryness to afford **4** (51.2 g, 77.0%) as a colorless oil.

^{1}H NMR (300 MHz, chloroform-*d*) δ 7.30 (q, *J* = 2.1 Hz, 1H), 7.28−7.24 (m, 1H), 7.15 (dd, *J* = 5.1, 1.3 Hz, 1H), 7.03 (d, *J* = 7.9 Hz, 1H), 6.96−6.87 (m, 1H), 6.72 (dq, *J* = 3.6, 1.2 Hz, 1H), 4.09 (s, 2H), 2.25 (s, 3H).

^{13}C NMR (75 MHz, chloroform-*d*) δ 142.47, 140.71, 135.28, 132.17, 132.00, 129.79, 126.90, 125.29, 124.03, 119.64, 33.54, 19.03.

Mass (HPLC-MS): 268.9 (M + 1).

*(3R,4S,5R,6R)-3,4,5-Tris((trimethylsilyl)oxy)-6-(((trimethylsilyl)-oxy)methyl)tetrahydro-2H-pyran-2-one (**5**).* Compound **5** was synthesized as described before.[24−26] Trimethylchlorosilane (82.3 g, 97 mL, 6 equiv, 758 mmol) was slowly added (over 40 min) via an addition funnel to a cold (−10 °C, salty iced water) mixture of (3*R*,4*S*,5*S*,6*R*)-3,4,5-trihydroxy-6-(hydroxymethyl)tetrahydro-2*H*-pyran-2-one (22.5 g, 1 equiv, 126 mmol) and *N*-methylmorpholine (102 g, 0.11 L, 8 equiv, 1.01 mol) in tetrahydrofuran (200 mL). The heterogeneous reaction mixture was stirred overnight from −10 to 25 °C. Toluene (300 mL) was added, and the white heterogeneous mixture was cooled down to 0 °C and brine was slowly added. The organic layer was washed successively with aqueous sodium phosphate (monobasic) and brine, then dried over sodium sulfate, filtered, and concentrated to afford a crude oil, which was stripped with toluene (3×) and heptane (1×). Intermediate **5** (61.0 g, 103%) was isolated as a yellow oil.

^{1}H NMR (300 MHz, chloroform-*d*) δ 4.17 (dt, *J* = 7.7, 2.5 Hz, 1H), 3.99 (d, *J* = 9 Hz, 1H), 3.90 (t, *J* = 9 Hz, 1H), 3.84-3.72 (m, 3H), 0.28−0.07 (m, 36H).

^{13}C NMR (75 MHz, chloroform-*d*) δ 170.94, 81.25, 75.81, 73.02, 70.73, 61.30, 0.73, 0.52, 0.23, −0.46.

*(3R,4S,5S,6R)-6-(Hydroxymethyl)-2-methoxy-2-(4-methyl-3-(thi-ophen-2-yl-methyl)phenyl)tetrahydro-2H-pyran-3,4,5-triol (**6**).* A solution of *n*-butyllithium (2.5 M in tetrahydrofuran) (6.78 g, 42 mL, 1.1 equiv, 106 mmol) was added at −78 °C to a solution of **4** (25.7 g, 1 equiv, 96.2 mmol) in tetrahydrofuran (250 mL), resulting in a yellow solution. After 30 min, the Li/Br exchange was complete according to HPLC. A solution of **5** (53.9 g, 1.2 equiv, 115 mmol) in tetrahydrofuran (80 mL) was added over 45 min at −78 °C to the reaction mixture, and the latter was stirred for 4 h at this temperature. Thin-layer chromatography (heptane/ethyl acetate (AcOEt) 95/5) showed almost full conversion of the Li-intermediate. A solution of methanesulfonic acid (27.7 g, 18.7 mL, 3 equiv, 289 mmol) in methanol (250 mL) was added at −78 °C to the reaction mixture over the course of 20 min (became almost colorless after 2/3 of the acidic mixture was added), and the cold bath was removed. The reaction mixture was stirred overnight at room temperature during which time it turned turbid and yellow. The reaction mixture was quenched with saturated aqueous sodium bicarbonate and extracted with AcOEt (3×). The organic layers were washed with brine (2×), dried over sodium sulfate, filtered, and concentrated to a brown oil. The latter was dissolved in a minimum of toluene and a drop of AcOEt and then precipitated by adding heptane. The solids were filtered, washed with heptane, and dried under reduced pressure to afford **6** (18 g, 49% yield) as an off-white solid. Proton NMR analysis indicated the presence of

https://doi.org/10.1021/acs.jmedchem.1c01269
J. Med. Chem. 2021, 64, 16641−16649

compound **6** as a mixture of diastereoisomers. The sugar part and methoxy group are clearly visible in the NMR spectrum, and the mixture was used as such in the next step.

*(2R,3R,4R,5S,6S)-2-(Acetoxymethyl)-6-(4-methyl-3-(thiophen-2-yl-methyl)phenyl)tetrahydro-2H-pyran-3,4,5-triyl Triacetate (**7**).*[27] $BF_3.OEt_2$ (20 g, 18 mL, 3 equiv, 0.14 mol) was slowly added (during 20 min) at 0 °C to a solution of **6** (18 g, 1 equiv, 47 mmol) and triethylsilane (17 g, 23 mL, 3 equiv, 0.14 mol) in a 1/1 mixture of DCM/ACN (180 mL) resulting in a brown homogeneous mixture. The latter was stirred at 0 °C for 1 h and then for 2 h at room temperature. The reaction mixture was cooled to 0 °C and quenched with saturated aqueous sodium bicarbonate. The aqueous layer was extracted with AcOEt (2×). Organic layers were washed with brine (2×), dried over sodium sulfate, filtered, and concentrated to afford a light brown foam (14.75 g, 42.09 mmol, 89% yield, many impurities present). The intermediate was then dissolved in DCM (150 mL), and 4-dimethylaminopyridine (514.2 mg, 0.1 equiv, 4.21 mmol), pyridine (33.29 g, 34 mL, 10 equiv, 420.9 mmol), and acetic anhydride (42.97 g, 39.8 mL, 10 equiv, 420.9 mmol) were successively added. The reaction mixture was stirred overnight at room temperature. The reaction mixture was partitioned between DCM and water. The aqueous layer was extracted with DCM (2×), and the organic layers were washed with 1 M hydrochloride (1×) and water (1×). The combined organic layers were dried over sodium sulfate, filtered, and concentrated to a brown oil. The residue was dissolved in a minimum amount of DCM and was purified by silica gel chromatography, eluting with a gradient from 10 to 25% AcOEt in heptane. The first fraction that contained α-anomer was discarded. The second fraction (4.5 g) that contained a mixture of α- and β-anomers was isolated to be repurified. The third fraction (6.5 g) that contained pure β-isomer was isolated. The second fraction was repurified by automated silica gel chromatography to afford another crop of pure β-anomer. Intermediate **7** was isolated as a white solid (8.5 g, 39% yield).

^{1}H NMR (300 MHz, chloroform-*d*) δ 7.23−7.08 (m, 4H), 6.89 (ddt, J = 5.1, 3.3, 1.5 Hz, 1H), 6.66 (dt, J = 3.2, 1.5 Hz, 1H), 5.37−5.15 (m, 2H), 5.19−5.05 (m, 1H), 4.39−4.21 (m, 2H), 4.21−4.02 (m, 3H), 3.82 (ddd, J = 10.0, 4.8, 2.4 Hz, 1H), 2.30−2.23 (m, 3H), 2.11−1.96 (m, 9H), 1.79−1.71 (m, 3H).

^{13}C NMR (75 MHz, chloroform-*d*) δ 170.72, 169.49, 138.38, 137.09, 134.13, 130.70, 128.51, 126.75, 125.34, 124.95, 123.74, 80.03, 76.06, 74.33, 72.64, 68.65, 62.40, 33.68, 20.76, 20.62, 20.38, 19.23.

*(2R,3R,4R,5S,6S)-2-(Acetoxymethyl)-6-(3-((5-(4-bromophenyl)-thiophen-2-yl)methyl)-4-methylphenyl)tetrahydro-2H-pyran-3,4,5-triyl Triacetate (**9**).* Bis(tricyclohexylphosphine)palladium(0) (0.4 g, 0.2 equiv, 0.6 mmol) was added to a degassed (5 min bubbling with nitrogen) mixture of **7** (2.0 g, 1 equiv, 3.9 mmol), 1,4-dibromobenzene (**8**) (9.1 g, 10 equiv, 39 mmol), potassium carbonate (2.1 g, 4 equiv, 15 mmol), and pivalic acid (0.39 g, 1 equiv, 3.9 mmol) in dimethylacetamide (30 mL). The reaction mixture was stirred for 18 h at 80 °C under a nitrogen atmosphere. After cooling to room temperature, the reaction mixture was diluted with AcOEt and then washed with aqueous ammonium chloride. The aqueous layer was extracted with AcOEt (2×). The organic layers were washed with aqueous ammonium acetate (1×) and brine (1×), dried over sodium sulfate, filtered, and concentrated to afford a crude brown solid. The solid was dissolved in a minimum amount of dichloromethane and purified by automated column chromatography. After concentration of the desired fraction, 0.9 g of a light yellow solid was isolated containing the desired product contaminated with a few impurities. The solid was therefore dissolved in a minimum amount of dimethyl sulfoxide (DMSO) and purified by normal phase chromatography (C18 silica gel). The product containing fraction was concentrated to dryness to afford **9** (0.80 g, 1.19 mmol, 31%) as a white solid.

^{1}H NMR (300 MHz, chloroform-*d*) δ 7.48−7.32 (m, 4H), 7.17 (tq, J = 5.4, 3.9, 2.7 Hz, 3H), 7.09 (d, J = 3.6 Hz, 1H), 6.62 (d, J = 3.6 Hz, 1H), 5.21 (ddd, J = 37.2, 18.2, 9.3 Hz, 3H), 4.36 (d, J = 9.8 Hz, 1H), 4.28 (dd, J = 12.3, 4.7 Hz, 1H), 4.15 (dd, J = 12.3, 2.3 Hz, 1H), 4.09 (s, 2H), 3.82 (ddd, J = 9.8, 4.8, 2.3 Hz, 1H), 2.29 (s, 3H), 2.02 (2 × s, 6H), 1.99 (s, 3H); 1.75 (s, 3H).

^{13}C NMR (75 MHz, chloroform-*d*) δ 170.71, 170.36, 169.50, 143.68, 137.97, 137.12, 134.25, 131.87, 130.78, 128.50, 126.88, 126.08, 125.60, 123.15, 79.99, 76.08, 74.32, 72.65, 68.63, 62.39, 34.03, 20.76, 20.66, 20.64, 20.41, 19.28.

(2R,3R,4R,5S,6S)-2-(Acetoxymethyl)-6-(4-methyl-3-((5-(4-(4,4,5,5-tetramethyl-1,3,2-dioxaborolan-2-yl)phenyl)thiophen-2-yl)methyl)phenyl)tetrahydro-2H-pyran-3,4,5-triyl Triacetate (Canagliflozin Precursor). (1,1′-Bis(diphenylphosphino)ferrocene)-palladium(II) dichloride (54 mg, 0.05 equiv, 74 μmol) was added to a degassed (5 min nitrogen bubbling) mixture of **9** (1.0 g, 1 equiv, 1.5 mmol), bispinacolatodiboron (0.75 g, 2 equiv, 3.0 mmol), and potassium acetate (0.19 g, 1.3 equiv, 1.9 mmol) in 1,4-dioxane (20 mL). The reaction mixture was stirred for 18 h at 100 °C under a nitrogen atmosphere. The reaction mixture was cooled to room temperature, quenched with brine, and extracted with toluene (3×). The organic layers were washed with brine, dried over sodium sulfate, filtered, and concentrated. The resulting dark oil (2 g) was dissolved in DMSO and purified by reverse phase chromatography (C18 silica gel). After concentration under reduced pressure, the canagliflozin precursor was isolated as a tan solid (915 mg, 1.27 mmol, 85% yield).

^{1}H NMR (300 MHz, chloroform-*d*) δ 7.75 (d, J = 7.8 Hz, 2H), 7.51 (d, J = 7.8 Hz, 2H), 7.22−7.12 (m, 4H), 6.64 (d, J = 3.6 Hz, 1H), 5.37−5.08 (m, 3H), 4.36 (d, J = 9.7 Hz, 1H), 4.28 (dd, J = 12.4, 4.7 Hz, 1H), 4.20−4.02 (m, 3H), 3.88−3.77 (m, 1H), 2.30 (s, 3H), 2.10−1.96 (m, 9H), 1.75 (d, J = 0.9 Hz, 3H), 1.37−1.31 (m, 12H).

^{13}C NMR (75 MHz, $CDCl_3$) δ 170.77, 170.39, 169.51, 168.85, 143.70, 142.53, 138.04, 137.17, 136.98, 135.28, 134.19, 130.82, 128.63, 126.01, 125.50, 124.50, 123.27, 83.79, 80.04, 77.43, 77.01, 76.58, 76.09, 74.34, 72.61, 68.64, 62.39, 34.07, 24.85, 20.77, 20.66, 20.64, 20.39, 19.29.

Mass (HPLC-MS): 738.0 (M + NH_4^+).

Radiochemistry. *Automated Synthesis.* The [^{18}F]canagliflozin production was performed in a Modular-Lab PharmTracer Eckert & Ziegler synthesis module. This synthesis module is equipped with disposable cassettes (6 valves and 18 valves, which is suitable for a GMP-based production of PET tracers (Supporting Information Figure S3)). Briefly, [^{18}F]fluoride was produced by the irradiation of ^{18}O-water with an IBA cyclotron via the ^{18}O(p, n)^{18}F nuclear reaction. The aqueous [^{18}F]fluoride was passed through a PS-HCO_3 anion-exchange cartridge (Synthra) to recover the ^{18}O-enriched water. The cartridge was washed with 1 mL of 2-propanol, and afterward, the [^{18}F]fluoride was eluted from the cartridge with 3 mg of tetraethylammonium bicarbonate (TEAHC) in 0.5 mL of 2-propanol and collected in a vial containing 13.8 mg of tetrakis(pyridine)copper(II) triflate ($Cu(OTf)_2(py)_4$) and 4 mg of canagliflozin precursor in 0.6 mL *N*,*N*-dimethylacetamide. The reaction mixture was heated at 140 °C for 20 min. Thereafter, the reactor was cooled to 40 °C and 0.5 mL of 1 M sodium hydroxide was added, and the mixture was allowed to react for 2 min. The mixture was then diluted with 0.3 mL of eluent (45% ACN/water, 0.1% TFA) and purified by HPLC (Prodigy Prodigy ODS-3 100 A 5 μm, 250 mm × 100 mm) with a flow of 4 mL/min. The radioactive product with a retention time of approximately 14 min was collected, diluted with 70 mL water, and applied to an OASIS 1 cc cartridge (Waters). The cartridge was washed with 2 × 7 mL of water, and the product was eluted with 1 mL of ethanol and 9 mL of 0.9% saline and transferred via a sterilization filter (Millex-LG filter, 0.2 μm pore size, polytetrafluoroethylene membrane, Millipore) to a sterile and pyrogen-free vial. Quality control was performed by ultraperformance liquid chromatography (UPLC), as described below.

Validation of Analytical Methods. To produce radiopharmaceuticals according to GMP regulations, quality control with validated analytical methods is required.[28] For the validation of the production of [^{18}F]canagliflozin, a UPLC method using an ACQUITY UPLC BEH C18 1.7 μm (2.1 mm × 50 mm) column was used, with both an isocratic and a gradient system. A significant difference in lipophilicity made it impossible to measure all known impurities with an isocratic method; however, with a gradient method, the matrix effect at 217 nm was significant, considering the low absorption coefficient of canagliflozin. Therefore, both systems were used and validated for retention times, linearity, precision, carry-over, recovery of [^{18}F]canagliflozin, quanti-

https://doi.org/10.1021/acs.jmedchem.1c01269
J. Med. Chem. 2021, 64, 16641−16649

fication and detection limits (LOQ and LOD), reproducibility and contribution from the matrix solution, and their corresponding acceptance criteria, as presented in Supporting Information Table S1. The isocratic eluted with a 35:65 aqueous ACN (0.1% TFA)/water (0.1% TFA) as mobile phase at a flow of 0.6 mL/min (λ = 217 nm, retention time: [^{18}F]fluoride = 0.5 min, [^{18}F]canagliflozin = 2.9 min). The gradient method used the same parameters but was ramped at 0 min with 10% ACN (0.1%TFA), 3 min with 30% ACN (0.1% TFA), 6 min with 60% ACN (0.1% TFA), and 8 min with 80% ACN (0.1% TFA).

All results were documented in a performance qualification (PQ) validation report, which was authorized by a qualified person (QP) before the validation of the production method was started.

Validation Production Method. To assure that the production method is robust and results in a product with consistent quality, validation of the production method was performed. Validation of [^{18}F]canagliflozin consisted of three independent productions, including complete quality control. All batch productions had to comply with the predefined acceptance criteria summarized in Table 1.

In Vitro Competition Experiments with Autoradiography. The use of human kidney tissues and the procedures for the in vitro experiments were performed according to the Dutch national ethical guidelines. The Medical Ethics Review Board of the University Medical Center Groningen judged that our study was exempt from Medical Research Involving Human Subjects Act (WMO). Visually healthy cortical parts of kidneys, removed because of renal cell carcinoma, were frozen and cut into 4 μm slices using a Leica CM 3050 cryostat (Leica Microsystems, Nussloch, Germany).

To assess specific binding, blocking experiments with canagliflozin and glucose were performed on slices incubated with [^{18}F]canagliflozin. To correlate [^{18}F]canagliflozin binding with SGLT2 distribution, IHC was performed on slices adjacent to the autoradiography slices incubated with the tracer.

Autoradiography. Kidney slices were incubated in [^{18}F]-canagliflozin (5 MBq in 50 mL) containing either alone phosphate-buffered saline (PBS) or PBS and canagliflozin (0.02 mM) or glucose (0.025 mM) for 60 min and then washed 3 times with cold PBS and 1 time with cold water. After drying by exposure to air for 20 min, the sections were exposed to a phosphor storage screen for 30 min. The exposed screens were then scanned, and images were analyzed.

Immunohistochemistry. The kidney slices were dried for 20 min using a cold blower and fixed with cold acetone for 10 min. After rinsing in PBS, the endogenous peroxidase was blocked with 0.015% H_2O_2 in PBS for 30 min. After rinsing in PBS, the samples were incubated with the primary SGLT2 antibody (polyclonal, raised in rabbit against amino acids 591−609 (ESAMEMNEPQAPAPSLFRQ-C) of the SGLT2 protein,[29] a gift from H Koepsell) (dilution 1:250 in PBS/1% BSA) for 60 min at room temperature. After rinsing in PBS, they were incubated with the secondary and third antibodies (horseradish peroxidase-labeled goat−antirabbit and rabbit−antigoat, respectively, from Dakopatts, Glostrup, Denmark, dilution 1:100 in PBS/1% BSA and 1% AB serum), both for 30 min at room temperature. After rinsing in PBS, the chromogenic reaction was visualized by incubation with 3-amino-9-ethylcarbazole Substrate Kit (Life Technologies) for 10 min. After rinsing in demineralized water, the slices were counterstained with hematoxyline (Fluka Chemie, Buchs, Switzerland), mounted in Kaiser's glycerol gelatin, and coverslipped. The IHC slices were scanned using a Hamamatsu NanoZoomer 2.0 HT slide scanner (Hamamatsu Photonics, Hamamatsu, Japan). Detailed images for this manuscript were created using NDPviewer 2.

Statistical Analysis. Data are expressed as mean ± standard deviation (SD). Two-tailed Welch's unequal variance *t*-test was used to compare the binding of [^{18}F]canagliflozin on autoradiography of kidney slices in the presence of canagliflozin or glucose relative to [^{18}F]canagliflozin alone. The significance level was set at $p < 0.05$.

■ ASSOCIATED CONTENT

Supporting Information

The Supporting Information is available free of charge at https://pubs.acs.org/doi/10.1021/acs.jmedchem.1c01269.

New synthesized compound full characterization (^{1}H and ^{13}C NMR), as well as the UPLC chromatograms of the precursor and canagliflozin confirming their purity (PDF)

Molecular formula strings, SMILE (CSV)

■ AUTHOR INFORMATION

Corresponding Author

Jasper Stevens − *Department of Clinical Pharmacy and Pharmacology, University of Groningen, University Medical Center Groningen, 9700 RB Groningen, The Netherlands*; Phone: +315036 17875; Email: j.stevens@umcg.nl; Fax: +31503614087

Authors

Sjoukje van der Hoek − *Department of Clinical Pharmacy and Pharmacology, University of Groningen, University Medical Center Groningen, 9700 RB Groningen, The Netherlands*; orcid.org/0000-0002-3186-9337

Inês F. Antunes − *Department of Nuclear Medicine and Molecular Imaging, University of Groningen, University Medical Center Groningen, 9700 RB Groningen, The Netherlands*; orcid.org/0000-0002-8003-5291

Khaled A. Attia − *Department of Nuclear Medicine and Molecular Imaging, University of Groningen, University Medical Center Groningen, 9700 RB Groningen, The Netherlands; Symeres, 9747 AT Groningen, The Netherlands*

Olivier Jacquet − *Symeres, 9747 AT Groningen, The Netherlands*

Andre Heeres − *Symeres, 9747 AT Groningen, The Netherlands; Hanze University of Applied Sciences, 9747 AS Groningen, The Netherlands*

Marian Bulthuis − *Department of Pathology and Medical Biology, Pathology Section, University of Groningen, University Medical Center Groningen, 9700 RB Groningen, The Netherlands*

Rolf Zijlma − *Department of Nuclear Medicine and Molecular Imaging, University of Groningen, University Medical Center Groningen, 9700 RB Groningen, The Netherlands*

Hendrikus H. Boersma − *Department of Clinical Pharmacy and Pharmacology, University of Groningen, University Medical Center Groningen, 9700 RB Groningen, The Netherlands*

Harry van Goor − *Department of Pathology and Medical Biology, Pathology Section, University of Groningen, University Medical Center Groningen, 9700 RB Groningen, The Netherlands*

Ton J. Visser − *Symeres, 9747 AT Groningen, The Netherlands*

Hiddo J. L. Heerspink − *Department of Clinical Pharmacy and Pharmacology, University of Groningen, University Medical Center Groningen, 9700 RB Groningen, The Netherlands*

Philip H. Elsinga − *Department of Nuclear Medicine and Molecular Imaging, University of Groningen, University Medical Center Groningen, 9700 RB Groningen, The Netherlands*; orcid.org/0000-0002-3365-4305

Complete contact information is available at: https://pubs.acs.org/10.1021/acs.jmedchem.1c01269

Author Contributions

S.v.d.H. and I.F.A. contributed equally. The manuscript was written through contributions of all authors. All authors have given approval to the final version of the manuscript.

Funding

The work described in this paper received funding from the Novo Nordisk Foundation, grant no. NNF OC0013659, and the Netherlands Organization for Health Research and Development, ZonMw, grant no. 459001018 (40-45900-98-119).

Notes

The authors declare no competing financial interest.

■ ABBREVIATIONS

ACN, acetonitrile; AcOEt, ethyl acetate; GMP, Good Manufacturing Practice; SGLT, sodium−glucose cotransporter; GLUT, glucose transporter; MTBE, methyl *tert*-butyl ether; UPLC, ultraperformance liquid chromatography

■ REFERENCES

(1) Amin, A. P.; Whaley-Connell, A. T.; Li, S.; Chen, S. C.; McCullough, P. A.; Kosiborod, M. N. The Synergistic Relationship between Estimated GFR and Microalbuminuria in Predicting Long-Term Progression to ESRD or Death in Patients with Diabetes: Results from the Kidney Early Evaluation Program (KEEP). *Am. J. Kidney Dis.* **2013**, *61*, S12−23.

(2) Wright, E. M.; Ghezzi, C.; Loo, D. D. F. Novel and Unexpected Functions of SGLTs. *Physiology* **2017**, *32*, 435−443.

(3) Zinman, B.; Wanner, C.; Lachin, J. M.; Fitchett, D.; Bluhmki, E.; Hantel, S.; Mattheus, M.; Devins, T.; Johansen, O. E.; Woerle, H. J.; Broedl, U. C.; Inzucchi, S. E. Empagliflozin, Cardiovascular Outcomes, and Mortality in Type 2 Diabetes. *N. Engl. J. Med.* **2015**, *373*, 2117−2128.

(4) Neal, B.; Perkovic, V.; Mahaffey, K. W.; De Zeeuw, D.; Fulcher, G.; Erondu, N.; Shaw, W.; Law, G.; Desai, M.; Matthews, D. R. Canagliflozin and Cardiovascular and Renal Events in Type 2 Diabetes. *N. Engl. J. Med.* **2017**, *377*, 644−657.

(5) Wiviott, S. D.; Raz, I.; Bonaca, M. P.; Mosenzon, O.; Kato, E. T.; Cahn, A.; Silverman, M. G.; Zelniker, T. A.; Kuder, J. F.; Murphy, S. A.; Bhatt, D. L.; Leiter, L. A.; McGuire, D. K.; Wilding, J. P. H.; Ruff, C. T.; Nilsson, G. I.; Fredriksson, M.; Johansson, P. A.; Langkilde, A. M.; Sabatine, M. S. Dapagliflozin and Cardiovascular Outcomes in Type 2 Diabetes. *N. Engl. J. Med.* **2019**, *380*, 347−357.

(6) Perkovic, V.; Jardine, M. J.; Neal, B.; Bompoint, S.; Heerspink, H. J. L.; Charytan, D. M.; Edwards, R.; Agarwal, R.; Bakris, G.; Bull, S.; Cannon, C. P.; Capuano, G.; Chu, P.-L.; de Zeeuw, D.; Greene, T.; Levin, A.; Pollock, C.; Wheeler, D. C.; Yavin, Y.; Zhang, H.; Zinman, B.; Meininger, G.; Brenner, B. M.; Mahaffey, K. W. Canagliflozin and Renal Outcomes in Type 2 Diabetes and Nephropathy. *N. Engl. J. Med.* **2019**, *380*, 2295−2306.

(7) Petrykiv, S. I.; Laverman, G. D.; de Zeeuw, D.; Heerspink, H. J. L. The Albuminuria-Lowering Response to Dapagliflozin Is Variable and Reproducible among Individual Patients. *Diabetes, Obes. Metab.* **2017**, *19*, 1363−1370.

(8) Scafoglio, C. R.; Villegas, B.; Abdelhady, G.; Bailey, S. T.; Liu, J.; Shirali, A. S.; Wallace, W. D.; Magyar, C. E.; Grogan, T. R.; Elashoff, D.; Walser, T.; Yanagawa, J.; Aberle, D. R.; Barrio, J. R.; Dubinett, S. M.; Shackelford, D. B. Sodium-Glucose Transporter 2 Is a Diagnostic and Therapeutic Target for Early-Stage Lung Adenocarcinoma. *Sci. Transl. Med.* **2018**, *10*, No. eaat5933.

(9) Bormans, G. M.; Van Oosterwyck, G.; De Groot, T. J.; Veyhl, M.; Mortelmans, L.; Verbruggen, A. M.; Koepsell, H. Synthesis and Biologic Evaluation of 11C-Methyl-D-Glucoside, a Tracer of the Sodium-Dependent Glucose Transporters. *J. Nucl. Med.* **2003**, *44*, 1075−1081.

(10) Sala-Rabanal, M.; Hirayama, B. A.; Ghezzi, C.; Liu, J.; Huang, S. C.; Kepe, V.; Koepsell, H.; Yu, A.; Powell, D. R.; Thorens, B.; Wright, E. M.; Barrio, J. R. Revisiting the Physiological Roles of SGLTs and GLUTs Using Positron Emission Tomography in Mice. *J. Physiol.* **2016**, *594*, 4425−4438.

(11) Nomura, S.; Sakamaki, S.; Hongu, M.; Kawanishi, E.; Koga, Y.; Sakamoto, T.; Yamamoto, Y.; Ueta, K.; Kimata, H.; Nakayama, K.; Tsuda-Tsukimoto, M. Discovery of Canagliflozin, a Novel C-Glucoside with Thiophene Ring, as Sodium-Dependent Glucose Cotransporter 2 Inhibitor for the Treatment of Type 2 Diabetes Mellitus (1). *J. Med. Chem.* **2010**, *53*, 6355−6360.

(12) Hummel, C. S.; Lu, C.; Liu, J.; Ghezzi, C.; Hirayama, B. A.; F Loo, D. D.; Kepe, V.; Barrio, J. R.; Wright, E. M. Structural Selectivity of Human SGLT Inhibitors. *Am. J. Physiol.: Cell Physiol.* **2012**, *302*, C373−C382.

(13) Ghezzi, C.; Yu, A. S.; Hirayama, B. A.; Kepe, V.; Liu, J.; Scafoglio, C.; Powell, D. R.; Huang, S.-C.; Satyamurthy, N.; Barrio, J. R.; Wright, E. M. Dapagliflozin Binds Specifically to Sodium-Glucose Cotransporter 2 in the Proximal Renal Tubule. *J. Am. Soc. Nephrol.* **2017**, *28*, 802−810.

(14) Meng, W.; Ellsworth, B. A.; Nirschl, A. A.; McCann, P. J.; Patel, M.; Girotra, R. N.; Wu, G.; Sher, P. M.; Morrison, E. P.; Biller, S. A.; Zahler, R.; Deshpande, P. P.; Pullockaran, A.; Hagan, D. L.; Morgan, N.; Taylor, J. R.; Obermeier, M. T.; Humphreys, W. G.; Khanna, A.; Discenza, L.; Robertson, J. G.; Wang, A.; Han, S.; Wetterau, J. R.; Janovitz, E. B.; Flint, O. P.; Whaley, J. M.; Washburn, W. N. Discovery of Dapagliflozin: A Potent, Selective Renal Sodium-Dependent Glucose Cotransporter 2 (SGLT2) Inhibitor for the Treatment of Type 2 Diabetes. *J. Med. Chem.* **2008**, *51*, 1145−1149.

(15) Ishiyama, T.; Murata, M.; Miyaura, N. Palladium(0)-Catalyzed Cross-Coupling Reaction of Alkoxydiboron with Haloarenes: A Direct Procedure for Arylboronic Esters. *J. Org. Chem.* **1995**, *60*, 7508−7510.

(16) Tredwell, M.; Preshlock, S. M.; Taylor, N. J.; Gruber, S.; Huiban, M.; Passchier, J.; Mercier, J.; Génicot, C.; Gouverneur, V. A General Copper-Mediated Nucleophilic 18F Fluorination of Arenes. *Angew. Chem., Int. Ed.* **2014**, *53*, 7751−7755.

(17) Ichiishi, N.; Brooks, A. F.; Topczewski, J. J.; Rodnick, M. E.; Sanford, M. S.; Scott, P. J. H. Copper-Catalyzed [18F]Fluorination of (Mesityl)(Aryl)Iodonium Salts. *Org. Lett.* **2014**, *16*, 3224−3227.

(18) Guibbal, F.; Isenegger, P. G.; Wilson, T. C.; Pacelli, A.; Mahaut, D.; Sap, J. B. I.; Taylor, N. J.; Verhoog, S.; Preshlock, S.; Hueting, R.; Cornelissen, B.; Gouverneur, V. Manual and Automated Cu-Mediated Radiosynthesis of the PARP Inhibitor [18F]Olaparib. *Nat. Protoc.* **2020**, *15*, 1525−1541.

(19) Taylor, N. J.; Emer, E.; Preshlock, S.; Schedler, M.; Tredwell, M.; Verhoog, S.; Mercier, J.; Genicot, C.; Gouverneur, V. Derisking the Cu-Mediated 18F-Fluorination of Heterocyclic Positron Emission Tomography Radioligands. *J. Am. Chem. Soc.* **2017**, *139*, 8267−8276.

(20) Wright, J. S.; Kaur, T.; Preshlock, S.; Tanzey, S. S.; Winton, W. P.; Sharninghausen, L. S.; Wiesner, N.; Brooks, A. F.; Sanford, M. S.; Scott, P. J. H. Copper-Mediated Late-Stage Radiofluorination: Five Years of Impact on Preclinical and Clinical PET Imaging. *Clin. Transl. Imaging* **2020**, *8*, 167−206.

(21) Preshlock, S.; Calderwood, S.; Verhoog, S.; Tredwell, M.; Huiban, M.; Hienzsch, A.; Gruber, S.; Wilson, T. C.; Taylor, N. J.; Cailly, T.; Schedler, M.; Collier, T. L.; Passchier, J.; Smits, R.; Mollitor, J.; Hoepping, A.; Mueller, M.; Genicot, C.; Mercier, J.; Gouverneur, V. Enhanced Copper-Mediated 18F-Fluorination of Aryl Boronic Esters Provides Eight Radiotracers for PET Applications. *Chem. Commun.* **2016**, *52*, 8361−8364.

(22) Clemente, G. S.; Zarganes-Tzitzikas, T.; Dömling, A.; Elsinga, P. H. Late-Stage Copper-Catalyzed Radiofluorination of an Arylboronic Ester Derivative of Atorvastatin. *Molecules* **2019**, *24*, No. 4210.

(23) Hummel, C. S.; Lu, C.; Loo, D. D. F.; Hirayama, B. A.; Voss, A. A.; Wright, E. M. Glucose Transport by Human Renal Na+/D-Glucose Cotransporters SGLT1 and SGLT2. *Am. J. Physiol.: Cell Physiol.* **2011**, *300*, C14−C21.

(24) Meng, W.; Ellsworth, B. A.; Nirschl, A. A.; McCann, P. J.; Patel, M.; Girotra, R. N.; Wu, G.; Sher, P. M.; Morrison, E. P.; Biller, S. A.; Zahler, R.; Deshpande, P. P.; Pullockaran, A.; Hagan, D. L.; Morgan, N.; Taylor, J. R.; Obermeier, M. T.; Humphreys, W. G.; Khanna, A.; Discenza, L.; Robertson, J. G.; Wang, A.; Han, S.; Wetterau, J. R.;

https://doi.org/10.1021/acs.jmedchem.1c01269
J. Med. Chem. 2021, 64, 16641−16649

Janovitz, E. B.; Flint, O. P.; Whaley, J. M.; Washburn, W. N. Discovery of Dapagliflozin: A Potent, Selective Renal Sodium-Dependent Glucose Cotransporter 2 (SGLT2) Inhibitor for the Treatment of Type 2 Diabetes. *J. Med. Chem.* **2008**, *51*, 1145−1149.
(25) Ohtake, Y.; Emura, T.; Nishimoto, M.; Takano, K.; Yamamoto, K.; Tsuchiya, S.; Yeu, S. Y.; Kito, Y.; Kimura, N.; Takeda, S.; Tsukazaki, M.; Murakata, M.; Sato, T. Development of a Scalable Synthesis of Tofogliflozin. *J. Org. Chem.* **2016**, *81*, 2148−2153.
(26) Deshpande, P. P.; Singh, J.; Pullockaran, A.; Kissick, T.; Ellsworth, B. A.; Gougoutas, J. Z.; Dimarco, J.; Fakes, M.; Reyes, M.; Lai, C.; Lobinger, H.; Denzel, T.; Ermann, P.; Crispino, G.; Randazzo, M.; Gao, Z.; Randazzo, R.; Lindrud, M.; Rosso, V.; Buono, F.; Doubleday, W. W.; Leung, S.; Richberg, P.; Hughes, D.; Washburn, W. N.; Meng, W.; Volk, K. J.; Mueller, R. H. A Practical Stereoselective Synthesis and Novel Cocrystallizations of an Amphiphatic SGLT-2 Inhibitor. *Org. Process Res. Dev.* **2012**, *16*, 577−585.
(27) Koga, Y.; Sakamaki, S.; Hongu, M.; Kawanishi, E.; Sakamoto, T.; Yamamoto, Y.; Kimata, H.; Nakayama, K.; Kuriyama, C.; Matsushita, Y.; Ueta, K.; Tsuda-Tsukimoto, M.; Nomura, S. C-Glucosides with Heteroaryl Thiophene as Novel Sodium-Dependent Glucose Cotransporter 2 Inhibitors. *Bioorg. Med. Chem.* **2013**, *21*, 5561−5572.
(28) Gillings, N.; Todde, S.; Behe, M.; Decristoforo, C.; Elsinga, P.; Ferrari, V.; Hjelstuen, O.; Peitl, P. K.; Koziorowski, J.; Laverman, P.; Mindt, T. L.; Ocak, M.; Patt, M. EANM Guideline on the Validation of Analytical Methods for Radiopharmaceuticals. *EJNMMI Radiopharm. Chem.* **2020**, *5*, No. 7.
(29) Vrhovac, I.; Eror, D. B.; Klessen, D.; Burger, C.; Breljak, D.; Kraus, O.; Radović, N.; Jadrijević, S.; Aleksic, I.; Walles, T.; Sauvant, C.; Sabolić, I.; Koepsell, H. Localizations of Na+-D-Glucose Cotransporters SGLT1 and SGLT2 in Human Kidney and of SGLT1 in Human Small Intestine, Liver, Lung, and Heart. *Pflugers Arch. Eur. J. Physiol.* **2015**, *467*, 1881−1898.

https://doi.org/10.1021/acs.jmedchem.1c01269
J. Med. Chem. 2021, 64, 16641−16649